Research Journal of Applied Sciences, Engineering and Technology 5(15): 3925-3933, 2013
DOI:10.19026/rjaset.5.4454
ISSN: 2040-7459; e-ISSN: 2040-7467

Submitted: August 29, 2012 Accepted: September 19, 2012 Published: April 25, 2013

Research Article

Planar Six-Element Ultra Wideband Array for Target Detection

[1]Baskaran Kasi and [2]Chandan Kumar Chakrabarty
[1]Department of Electrical and Electronics Engineering, Kuala Lumpur Infrastructure University College,
[2]Department of Electronics and Communication Engineering, Universiti Tenaga Nasional,
Kajang, Selangor 43000, Malaysia

Abstract: This study presents a planar Ultra-Wide Band (UWB) antenna array based on six identical UWB antenna elements. The feed network for the proposed structure is realized with Wilkinson power dividers. Dolph-Chebyshev distribution has been used to provide tapered feeding for the radiating elements. The fabricated array, with a compact size of 200 × 90 mm^2, operates over the frequency band from 3.8 to 10 GHz with a return loss less than –10 dB. Moreover, the measured peak gains of the array range from 5.5 to 10.8 dBi against the frequency. The experimented and simulated results are in good agreement. A time domain study has been performed to assess the suitability of the designed array for UWB applications.

Keywords: Dolph-Chebyshev distribution, micro strip fed-line, planar antenna array, time-domain characterization, ultra wideband systems, Wilkinson power divider

INTRODUCTION

Ultra Wide Band (UWB) radio technology has gained popularity in wireless communications, owing to its attractive features, such as low complexity, low cost and very high data rates. This license free technology was approved by the Federal Communications Commission (FCC, 2002). According to the FCC regulations, the radio frequency spectrum between 3.1 and 10.6 GHz can be used for commercial UWB activities. For this reason, there has been a surge of interest in the designing and development of UWB subsystems. The development of an optimal antenna is a challenge for the implementation of UWB radio systems. In this sense, the most promising candidate proposed for practical UWB applications is printed antennas. Such an antenna has a low profile, lightweight, ease of fabrication and a versatile integration with other microwave devices (James and Hall, 1989; Balanis, 2005).

A variety of omni-directional antennas for UWB applications have been reported recently (Koohestani and Golpour, 2010; Ahmed and Sebak, 2011; Yang and Yoshitomi, 2012). The broad-beam coverage in this type of antenna would be more favourable in mobile applications. Certain modern electronic devices such as radar systems, localization systems and microwave imaging for cancer screening, however, require a very good directional and high gain antenna. As inferred from the literature, a typical UWB antenna element will have a low gain of order 3 to 4 dBi. Therefore, it appears reasonable to consider familiar method like arrays to enhance the gain or to provide beam scanning capability. Several studies have been carried out to investigate the characteristics of UWB planar antenna array. In literature (Li *et al*., 2006; Adamiuk *et al*., 2009), it was noted that the feed networks of the array are not embedded with the radiating elements thus posing a challenge for designers to integrate them into small electronic devices. Chen and Wang (2008) in their recent study have integrated the feed network into an array of antennas, but have not shown the experimental results of their work. In (Chen and Wang, 2010; Huang and Xu, 2010), the authors have presented experimental results of their proposed UWB arrays, but did not investigate the method to suppress the side lobe level of the arrays. One of the important issues in designing arrays is the mutual coupling between elements. The effect of this phenomenon on the antenna array design has to be kept as minimum as possible to prevent distortion in the transmitted signal.

This study proposes a six-element planar UWB antenna array. Its characteristics are investigated numerically and validated experimentally.

ANTENNA ELEMENT AND PARAMETRIC STUDY

Figure 1 illustrates the proposed geometry of the antenna. The antenna is located in the *x*–*y* plane and the normal direction is *z*-axis. The radiator and the feeding structure are printed on a standard Taconic TLC–30

Corresponding Author: Baskaran Kasi, Department of Electrical and Electronics Engineering, Kuala Lumpur Infrastructure University College, Kajang, Selangor 43000, Malaysia

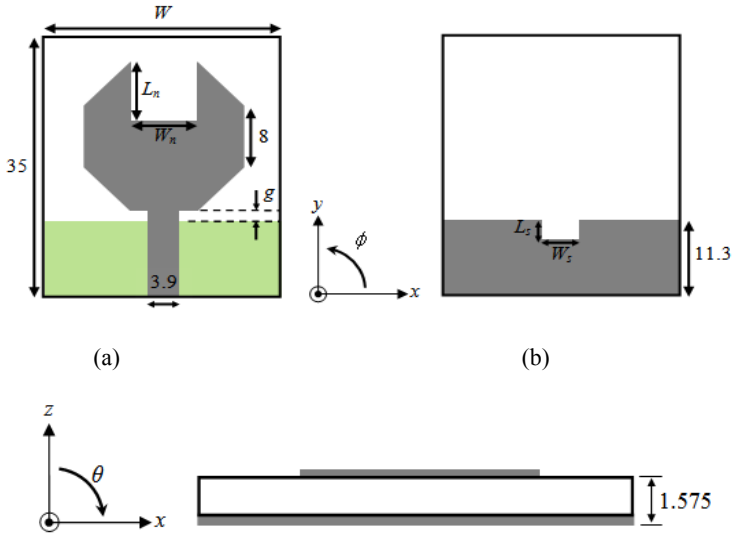

Fig. 1: Geometry of the proposed UWB antenna (Units in mm). (a)Front view, (b) Rear view, (c) Side view

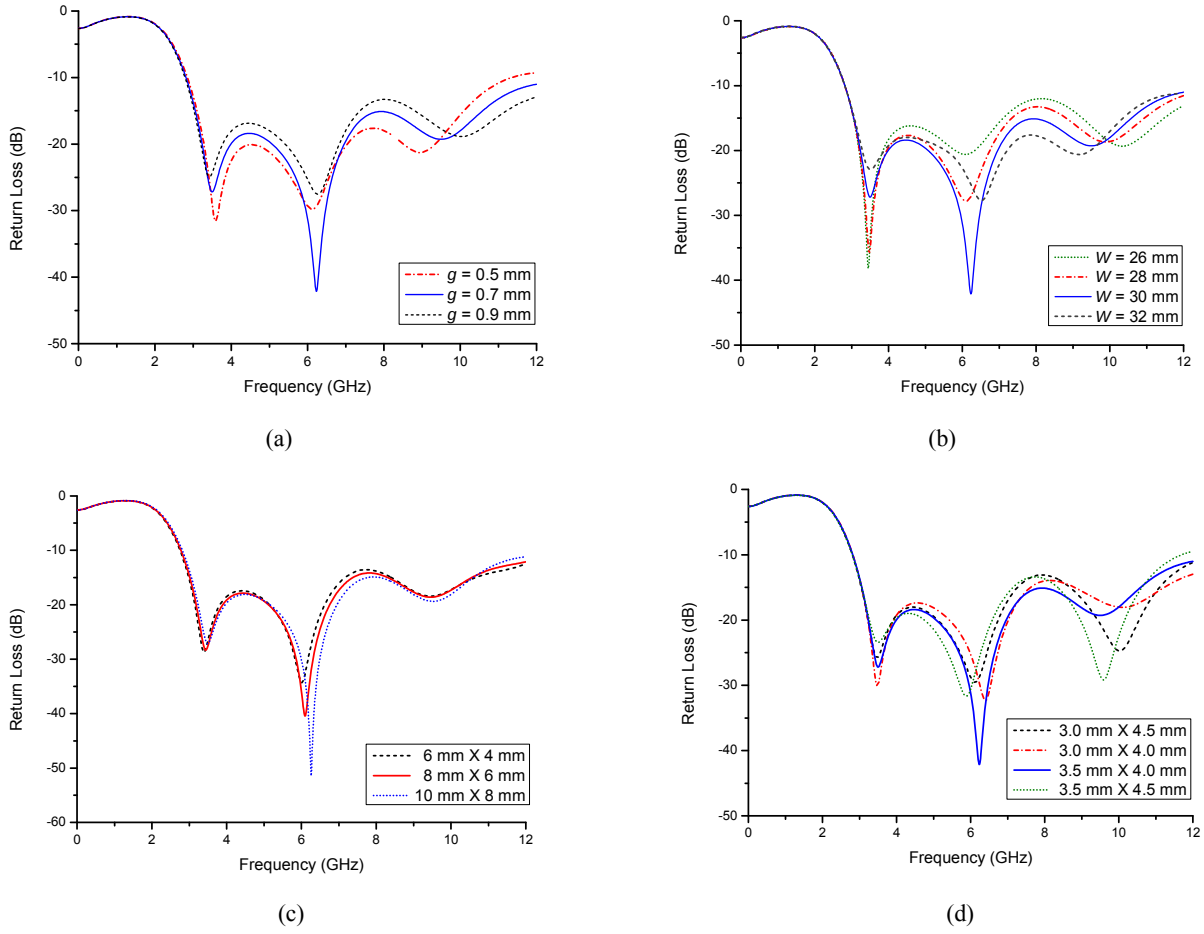

Fig. 2: Parametric study. (a) Feed gap size, (b) Ground plane width, (c) Notch cut and (d) Rectangular slot size

substrate with a height of 1.575 mm and relative permittivity of 3.0. As it is given in Fig. 1, the antenna consists of a beveled shape rectangular patch and is connected to a microstrip line. The microstrip feed line has a characteristic impedance of 50 Ω and terminated with a standard subminiature version A (SMA) connector. On the other side of the dielectric substrate, a truncated ground plane is printed below the microstrip feed line.

Various broad-banding techniques have been suggested by researchers to enhance the performance of microstrip antenna (Wong, 2002). Three techniques have been adopted in this paper to enhance the impedance bandwidth of the proposed antenna. Firstly, a bevel-shaped patch is applied. Then, a U-shape slot of suitable dimensions is cut on the radiator to enhance and obtain the impedance bandwidth. The third technique is to embed a notch structure on the ground plane of the antenna. A parametric study of the proposed antenna is carried out in order to achieve UWB operation. To fully understand the influence of these parameters on the operating bandwidth, only one parameter is considered at a time while the others were kept constant as shown in Fig. 1. The antenna parameters are tuned by simulation using CST Microwave Studio commercial software.

Feed gap separation *g*: The feed gap is the distance between the radiator and the ground plane. This parameter affects the impedance characteristic of the antenna and is denoted with *g* in Fig. 1. Variation of return losses of the antenna for different feed gap values is shown in Fig. 2a. The plots show that by decreasing *g*, the return loss response improves (between 3.5-5.8 GHz and 7.0-9.5 GHz); but the impedance bandwidth of the antenna decreases. The optimum value of feed gap is found to be 0.7 mm, which gives the lowest return loss level in the UWB band.

Ground plane width *W*: The other critical design parameter that governs the impedance bandwidth of the proposed antenna is the ground plane width. The dimension of the ground plane width is demonstrated in Fig. 1 by *W*. Fig. 2b displays the return loss curves for various values of *W*. It can be observed that the second resonance shifts from 5.8 to 6.6 GHz with an increase in the width of *W* from 26 to 32 mm and there is no affect of width change on the first resonance frequency located at 3.5 GHz. The best performance is obtained with optimized *W* of 30 mm.

Notch cut on the radiator (L_n and W_n): The dimensions of the notch cut are depicted in Fig. 1 by L_n and W_n. The effect of the notch cut dimensions on the antenna's performance is illustrated in Fig. 2c. It can be seen clearly that the return loss curves nearly remain the same with the variation of the notch size; however the second resonance frequency shift slightly. It is noticeable that the antenna impedance characteristic is almost independent of the notch cut dimensions.

Table 1: Parameter values of the fabricated antenna

Parameter	W	W_n	L_n	W_s	L_s	g
Value (mm)	30	8	8	4	3.5	0.7

Fig. 3: Photograph of fabricated antenna

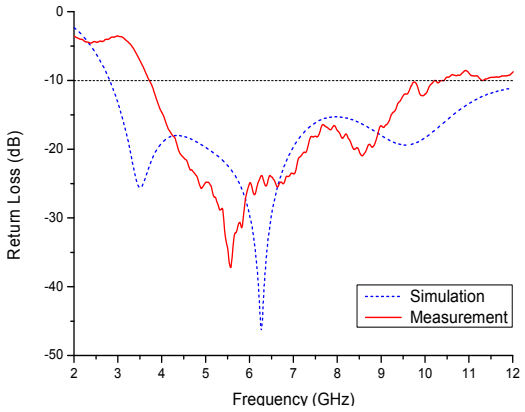

Fig. 4: Simulated and measured return loss of the proposed antenna

Truncated ground plane rectangular notch (L_s and W_s): Figure 2d illustrates the return loss curves of the antenna for various values of L_s and W_s and it is also clearly shows how the second and third resonance frequencies change remarkably when the slot size is varied from 3 mm×4 mm to 3.5 mm×4.5 mm. It is also noticed that, the first resonance stays around 3.5 GHz with variation in L_s and W_s. The rectangular notch dimensions therefore, would influence the antenna performance both in the mid-band and the upper band.

In the parametric study process, four salient parameters have been investigated numerically to attain a wider impedance bandwidth for the proposed element and the results of the investigation help engineers to select the optimum parameter values for the practical prototype. The proposed UWB printed antenna is

fabricated using the optimized parameter values given in Table 1 and the photograph is shown in Fig. 3.

To validate the proposed design, the fabricated antenna was measured using a Rhode and Schwarz® ZVL network analyzer. The simulated and measured return loss curves of the prototype are plotted and compared with each other in Fig. 4. The predicted 10 dB return loss band width is from 2.8 to 12.0 GHz whereas its measured return loss bandwidth is from 3.8 to 10.4 GHz. A reasonable match has been found between calculated and measurement results. The slight differences between the two plots can be attributed to the effect of SMA connector and fabrication tolerance.

Two principal orthogonal planes are selected to represent the simulated far-field radiation patterns of the proposed antenna. The normalized radiation patterns in both the *H*–plane (*x*–*z* plane) and *E*–plane (*y*–*z* plane) have been examined at various frequencies as shown in Fig. 5. The results clearly show a stable unidirectional pattern in the *H*–plane and a quasi-unidirectional pattern in the *E*-plane.

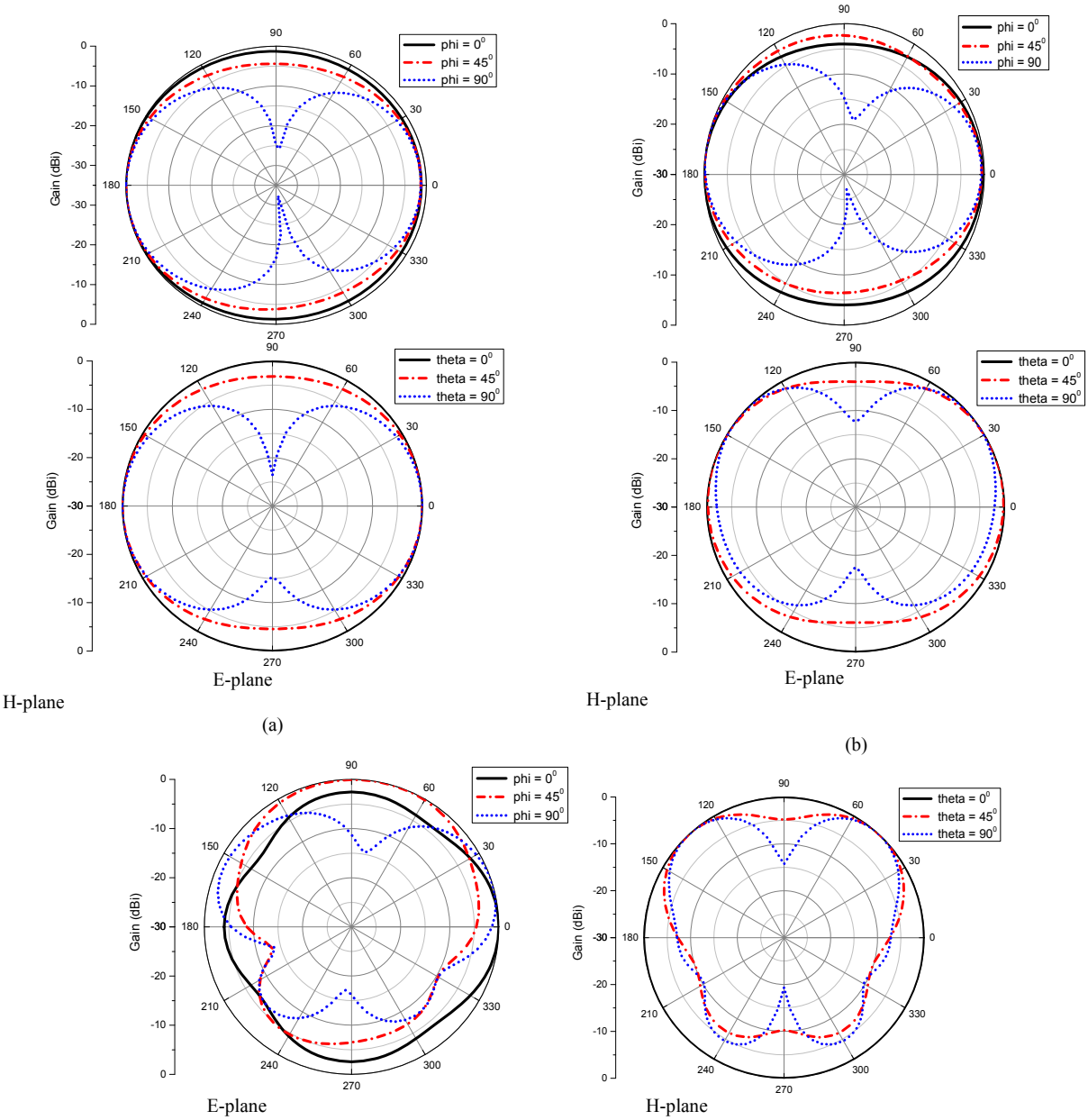

Fig. 5: Simulated *E* – plane and *H* – plane radiation patterns for the proposed antenna at (a) 3 GHz, (b) 6 GHz and (c) 9 GHz

ARRAY

It is well known that application such as target detection demands directional antenna with high gain as well as beam steering capability. A single antenna element may not be able to meet such requirements. Thus, an antenna array seems to be a good candidate to resolve this problem. Traditionally, linear antenna arrays are designed to produce a narrow beam pattern. The most straightforward approach to achieve such a narrow main beam is to increase the number of antenna array elements. However this approach dramatically increases the overall array size and leads to complex fabrication process. On the other hand, the increment of distance among the resonating elements can be an alternative technique to achieve a pencil beam shape radiation pattern. Despite increasing the array's directivity, this method may contribute to additional side lobes and undesirable grating lobes. This can be solved by incorporating tapered amplitude distribution in antenna arrays. However, the grating lobes reduction of the array by amplitude tapering lead to a more broadened main beam. In other words, the engineer who intends to design an antenna array has to compromise between the beamwidth and the side lobe level. As suggested in (Milligan, 2005), the most popular tapered distributions used to suppress the side lobe level in antenna arrays are binomial, triangular, Dolph–Chebyshev and Taylor.

Power dividers are one of the essential elements in the construction of feeding networks for the antenna array. In the present work, an ultra-wideband power divider should be constructed and used in the feed network. The Wilkinson power divider (WPD) was invented in 1960 (Wilkinson, 1960) and has wide applications in microwave circuits and antenna feeds because of its convenient design and good performance. It is worth mentioning here that the WPD can be designed with arbitrary output power distribution ratio. However, one drawback of the conventional WPD is it operates only at one design frequency and therefore unsuitable for UWB applications. To address this problem, a number of UWB WPD structures have been reported in the recent publications. These can be classified into two categories: two–way and three-way splitters. In the two-way power splitters, applications of multiple quarter wave transformers (Yang and Chu, 2008), radial stub (Ahmed and Sebak, 2009), overlapped butterfly radial stub (Zhou *et al*. 2010a) and delta stub (Zhou *et al*. 2010b) were shown to provide the desired UWB frequency response. On the other hand, in the three-way power distribution, a number of techniques have been proposed to achieve the UWB performance such as multilayer broadside coupling structure (Abbosh, 2007; 2008; 2012) and band notched using two-symmetrical F-shaped defected ground structure (Zhang *et al*., 2010).

The geometry of the proposed antenna array is shown Fig. 6. The array is composed of six identical radiators, as the one shown in Fig. 1 and connected by a feeding network. In order to attain a side lobe level−24 dB, the input signals of the antenna array have been tapered using an appropriate Dolph-Chebyshev window function. Table 2 summarizes the Dolph-Chebyshev excitation coefficients of each of the array elements.

The proposed feeding network consists of two parts: (1) an equal three-way UWB WPD used to obtain a-4.77 dB split ratio and (2) equal/unequal two-way

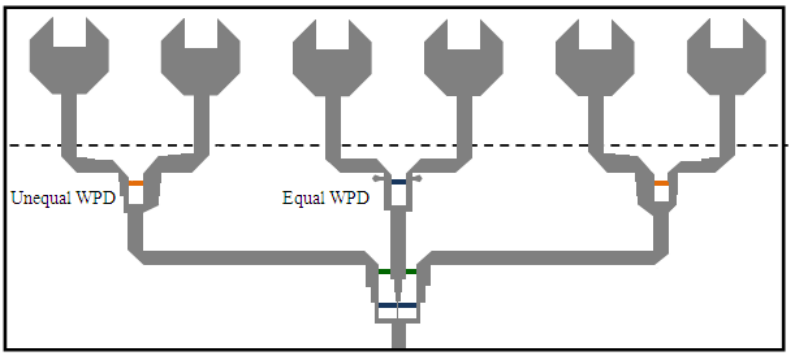

Fig. 6: Geometry of the proposed array

Table 2: Dolph-Cheybshev excitation amplitudes of the array elements

Element number	1	2	3	4	5	6
Normalized coefficients	0.411	0.736	1.000	1.000	0.736	0.411

UWB WPDs to feed the individual patches with tapered signals. The design centre frequency is 7 GHz. The 4.77 dB stage of the UWB feed network is designed based on the basic idea presented in (Zhang *et al*., 2010). For the first two elements of the array, an unequal two-way UWB WPD is used to achieve the required distribution. This power splitter has been derived based on (Pozar, 2005).

The detail design consideration for the equal two-way UWB power divider which is utilized to excite the radiator 3 and 4 are discussed in (Ahmed and Sebak, 2009). It is worth noting that the signals used to excite the last two elements are identical to that of the first two elements due to the fact that feed network is symmetrical. In the proposed array, at the design frequency of 7 GHz the distance between the patches is $0.79\lambda_0$ and the area is 200×90 mm^2.

SIMULATION AND MEASUREMENT RESULTS

The simulated *S*-parameters of the feed network are plotted in Fig. 7. As depicted in the figure, the simulated return loss is less than –10 dB from 3.5 to 12 GHz. For the first two elements of the array, the power distribution ratio should be of approximately 2 to 1. The transfer parameter S_{21} is equal to (–10 ± 1) dB across the band from 3 to 8 GHz. On the other hand, the insertion loss S_{31} is around (–7 ± 1) dB from 3 to 8 GHz. For the equal UWB power divider, the insertion loss is calculated as –7.8 dB. The simulated value falls within the (±0.6) dB margin of error as compared to the calculated value. A prototype of the proposed antenna array has been fabricated using the standard photolithography technique and is shown in Fig. 8. The predicted and measured return loss curves of the proposed six-element array are plotted in Fig. 9. The simulated -10 dB return loss bandwidth of the array is from 3.5 to 12.0 GHz, whereas its measured return loss bandwidth is from 3.8 to 10 GHz. Although there is a reasonable agreement between the experimental and simulated results, a slight variation is seen which may be due to the fabricating errors in constructing the antenna array.

Figure 10 plots the normalized *H*–plane radiation patterns of the array antenna at various frequencies. It is obvious that the radiation pattern of the array at 3 GHz has achieved a side lobe level of −6 dB as depicted in Fig. 10a. From Fig. 10b, it can be seen that the designed array has a good directional pattern with a side lobe suppression of 11 dB and 12.4^0 half power beam width at 7 GHz. On the other hand, the side lobe level of the energy pattern is higher than the main beam in Fig. 10c. This undesirable beam radiation is known as grating lobe.

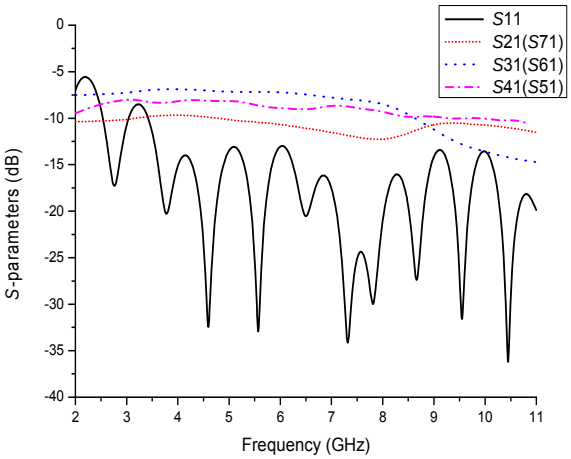

Fig. 7: Simulated *S*-parameters of the feed network

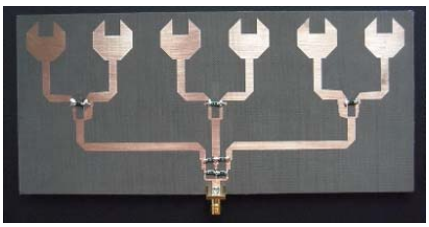

Fig. 8: Fabricated antenna array

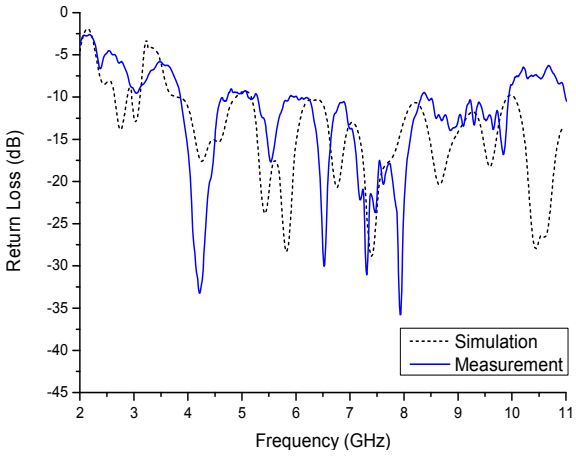

Fig. 9: Return loss of array

Figure 11 shows the measured gain at boresight (θ = 0°, ϕ = °0) for the antenna element and the array. It is seen that the antenna element gain varies from 2.2 to 4.2 dBi across the UWB frequency region. In case of the array, the gain steadily increases with frequency and reaches a maximum of 10.8 dBi at 7 GHz. Thereafter, it reduces gradually to 6.6 dBi because of mutual coupling effect between the feed lines.

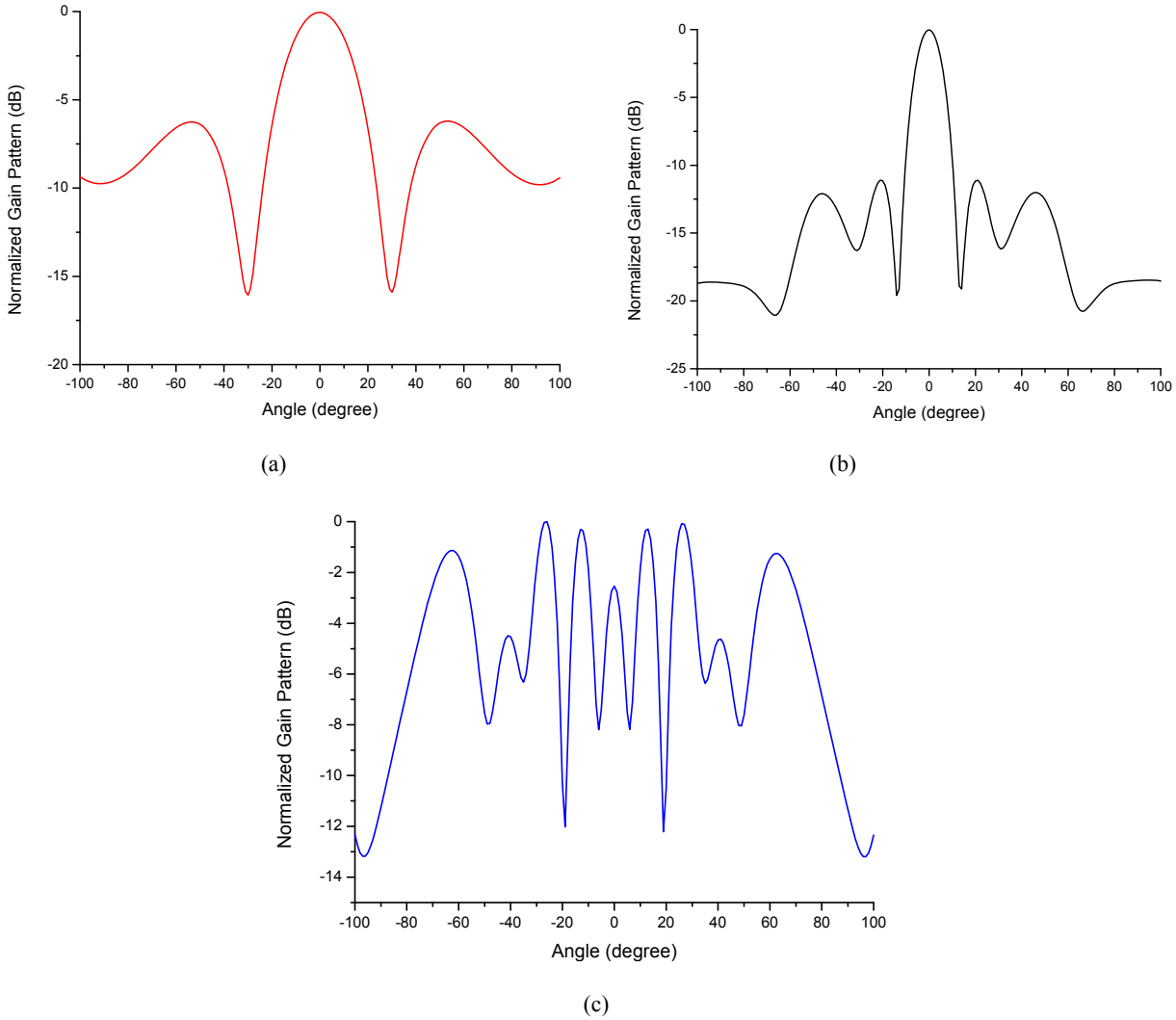

Fig. 10: Calculated radiation pattern of the antenna array in *H*-plane at (a) 3 GHz, (b) 7 GHz and (c) 10 GHz

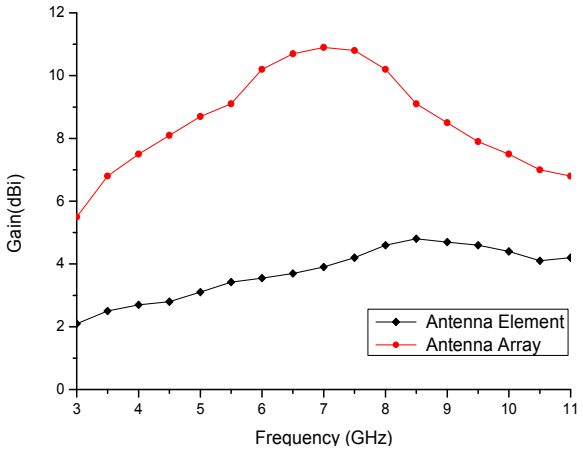

Fig. 11: Measured gains of single element and arrays at bore sight

TIME DOMAIN RESPONSE

The frequency domain results in the previous section are very encouraging. However, for impulse-based UWB radio technology, the radiated pulse shape should not be distorted by the antenna array. Therefore, it is not sufficient to evaluate the proposed array performance solely based on parameters such as input impedance, radiation pattern and gain. Instead, it is important to examine the time-domain response of the designed array in order to assess its suitability for UWB systems. For this purpose, a fifth-order Gaussian mono-pulse has been chosen as the excitation signal and is given by:

$$s_1(t) = GM_5(t) = \frac{Ae^{-t^2/2\sigma^2}}{\sqrt{2\pi}}\left(-\frac{t^5}{\sigma^{11}} + \frac{10t^3}{\sigma^9} - \frac{15t}{\sigma^7}\right) \quad (1)$$

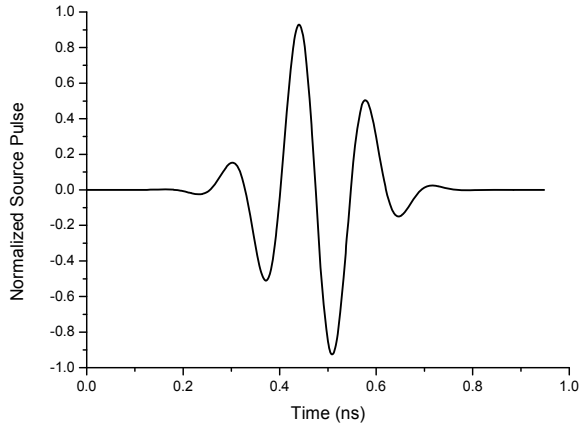

Fig. 12: Normalized antenna input pulse

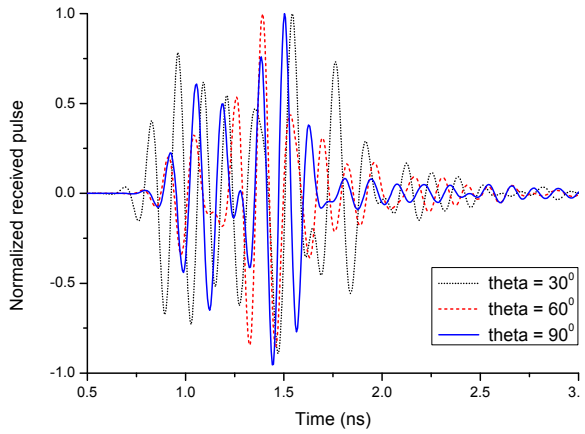

Fig. 13: Received pulse signals for various elevation angles

Table 3: Fidelity factor of the designed array

Angle, θ	Fidelity, F
30^0	0.8986
60^0	0.9260
90^0	0.8853

where A is a constant chosen to satisfy the limitation set by FCC and pulse width factor σ equals 51 ps to ensure that the shape of the spectrum complies with the spectral mask. The input signal is shown in Fig. 12.

Signal fidelity can be defined as the correlation coefficient between normalized input and output pulses. For two identical signal waveforms, the fidelity should be 1. A low fidelity between the source and received pulse indicates that the distortion in received pulses is high. In order to investigate the fidelity of the radiated signal, a virtual probe is placed in the far field of the antenna array. Figure 13 presents simulated pulse waveforms in elevation plane at selective angular locations of 30^0, 60^0 and 90^0. By comparing the normalized plots in Fig. 13, it is interesting to note that the radiated pulses are almost identical at all of the designated locations. The slight distortion exhibited in the received electrical pulse might be because of the ringing effect of the excitation pulse.

To determine the correlation coefficient between the received signal $s_2(t)$ and the source pulse $s_1(t)$, the following equation is used:

$$F = \max_{\tau} \left\{ \frac{\int_{-\infty}^{\infty} s_1(t) s_2(t-\tau)\, dt}{\sqrt{\int_{-\infty}^{\infty} s_1^2(t)\, dt} \sqrt{\int_{-\infty}^{\infty} s_2^2(t)\, dt}} \right\} \quad (2)$$

where, t is a delay and is varied to make the numerator in (2) a maximum value (Allen *et al*., 1993; Lamensdorf and Susman, 1994). The fidelity factor between the source pulse and the received pulse for the three elevation angles are summarized in Table 3.

The fidelity for the array ranges between 0.89 and 0.93. These results indicate that the proposed array antenna can produce the desired radiation patterns and also the short pulses of good quality.

CONCLUSION

This study begins by describing the implementation of a compact microstrip antenna element for UWB applications. The proposed radiating element has achieved good impedance matching, stable radiation patterns and consistent gain over the operating frequency band of 3 to 12 GHz. Then the authors designed a planar UWB antenna array system with six identical antenna elements and feed network. A gain variation between 5.5 and 10.8 dBi is measured between 3 and 7 GHz for the proposed array. As such with its good pulse handling characteristic, the presented array antenna is very well suited to UWB target detection applications.

ACKNOWLEDGMENT

The authors thank Mr. Fauzi Kadir for the construction of the prototypes. The authors would like to acknowledge Taconic Corporation, Republic of Korea, for providing the microwave substrate sample used in this study.

REFERENCES

Abbosh, A.M., 2007. A compact UWB 3-way power divider. IEEE Microw. Wirel. Compon. Lett., 17(8): 598-600.

Abbosh, A.M., 2008. Design of Ultra-Wide Band 3-way arbitrary power dividers. IEEE Trans. Microw. Theory Tech., 56(1): 194-20.

Abbosh, A.M., 2012. Ultra-Wide Band 3-way power divider using broadside coupled microstrip-coplanar waveguide. Microw. Opt. Tech. Lett., 54(1): 196-199.

Adamiuk, G., M. Janson, W. Wiesbeck and T. Zwick, 2009. Dual-polarized UWB antenna array. IEEE International Conference on Ultra-Wideband (ICUWB), September 9-11, Vancouver, Canada, pp: 159-163.

Ahmed, O. and A.R. Sebak, 2009. A modified Wilkinson power divider/combiner for ultra-wideband communications, IEEE Antennas and Propagation Society International Symposium, June 1-5, South Carolina, USA, pp: 1- 4.

Ahmed, O. and A.R. Sebak, 2011. A novel printed monopole antenna for future Ultra-Wide Band communication systems. Micro. Opt. Tech. Lett., 53(8): 1837-1841.

Allen, O.E., D.A. Hill and A.R. Ondrejka, 1993. Time-domain antenna characterizations, IEEE Trans. Electromag. Compat., 35(3): 339-346.

Balanis, C.A., 2005. Antenna Theory: Analysis and Design. 3rd Edn., John Wiley and Sons, Inc., New Jersey.

Chen, M. and J. Wang, 2008. Planar UWB antenna array with CPW feeding network, Asia-Pacific Microwave Conference (APMC), December 16-20, Hong Kong, China., pp: 1-4.

Chen, M. and J. Wang, 2010. Planar UWB antenna array with microstrip feeding network, IEEE International Conference on Ultra-Wide Band (ICUWB), September 20-23, Nanjing, China., pp: 1-3.

FCC, 2002. The 1st report and order regarding Ultra-Wide Band transmission systems. FCC 02-48, ET Docket, pp: 98-153.

Huang, B. and Y. Xu, 2010. Analysis and design of a novel UWB antenna array. International Conference on Microwave and Millimeter Wave Technology (ICMMT), May 8-11, Chengdu, China, pp: 313 – 316.

James, J.R. and P.S. Hall, 1989. Handbook of Microstrip Antennas, Peter Periginus Ltd., London.

Koohestani, M. and M. Golpour, 2010. U-shaped microstrip patch antenna with novel parasitic tuning stubs for ultra wideband applications. IET Microwaves Antennas Propagat., 4(7): 938-946.

Lamensdorf, D. and L. Susman, 1994. Baseband-pulse-antenna techniques, IEEE Antennas Propagat. Mag., 36(1): 20-30.

Li, P., J. Liang, X. Chen and C. Parini, 2006. A 4-element Ultra-Wide Band tapered-slot-fed antenna array. IEEE Antennas Propagat., July 9-14, New Mexico, USA.

Milligan, T.A., 2005. Modern Antenna Design. John Wiley and Sons, Inc., New Jersey.

Pozar, D.M., 2005. Microwave Engineering. 3rd Edn., John Wiley & Sons, Inc., New Jersey.

Wilkinson, E.J., 1960. An N-way hybrid power divider. IRE Trans. Microw. Theory Tech., 8 (1): 116-118.

Wong, K.L., 2002. Compact and Broadband Microstrip Antennas. John Wiley and Sons, Inc., New York.

Yang, L. and Q.X. Chu, 2008. Design of a compact UWB Wilkinson power divider. International Conference on Microwave and Millimeter Wave Technology (ICMMT), April 21-24, Nanjing, China., pp: 360-362.

Yang, L. and K. Yoshitomi, 2012. A compact circular corner monopole antenna for UWB application. Microw. Opt. Tech. Lett., 54(1): 147-150.

Zhang, Z., Y.C. Jiao, S. Tu, S.F. Cao and F.S. Zhang, 2010. Design of a 5.8 GHz band-notched UWB 3-way power divider using symmetric F-shaped DGS. International Symposium on Signals, Systems and Electronics (ISSSE), September 17-20, Nanjing, China., pp: 1-3.

Zhou, B., H. Wang and W.X. Sheng, 2010a. A novel UWB Wilkinson power divider, The 2nd International Conference on Information Science and Engineering (ICISE), December 4-6, Hangzhou, China., pp: 1763- 1765.

Zhou, B., H. Wang and W.X. Sheng, 2010b. A modified UWB Wilkinson power divider using delta stub. Prog. Electromag. Res. Lett., 19: 49-55.